

Walking cavity solitons

Dmitry V. Skryabin¹ and Alan R. Champneys²

¹*Department of Physics and Applied Physics, University of Strathclyde, Glasgow G4 0NG, United Kingdom*

²*Department of Engineering Mathematics, University of Bristol, Bristol BS8 1TR, United Kingdom*

(Received 17 November 2000; revised manuscript received 20 February 2001; published 24 May 2001)

A family of walking solitons is obtained for the degenerate optical parametric oscillator below threshold. The loss-driven mechanism of velocity selection for these structures is described analytically and numerically. Our approach is based on understanding the role played by the field momentum and generic symmetry properties and, therefore, it can be easily generalized to other dissipative multicomponent models with walk off.

DOI: 10.1103/PhysRevE.63.066610

PACS number(s): 42.65.Tg, 42.65.Ky

For multicomponent optical fields, the complexity of the problem of soliton formation is often enhanced by the difference between group velocities of the interacting components or double refraction properties of the nonlinear medium, which introduce, respectively, temporal and spatial walk off. Therefore, for existence of multicomponent mutually trapped solitons, intrinsic walk-off compensating mechanisms should be present in the problem along with more conventional diffraction or group velocity dispersion compensations. In the context of free propagation, walking solitons have recently been predicted theoretically [1–4] and observed experimentally [5,6] in degenerate and nondegenerate three-wave mixing in $\chi^{(2)}$ media [1–3,5,6] and in degenerate four-wave mixing in $\chi^{(3)}$ media [4]. Both of these systems are described by Hamiltonian conservative models.

Non-Hamiltonian systems with gain and loss also have paramount importance in nonlinear optics and the study of dissipative localized structures is a subject of much current research. A particularly important class of dissipative localized structures with potential for practical application are cavity solitons existing in optical cavities filled with passive nonlinear media and supported by external driving [7,8]. One of the possible advantages of using quadratic cavity solitons for information processing is that $\chi^{(2)}$ nonlinearity has a practically instantaneous response, while relatively large nonlinear coefficients can be achieved using modern phase matching techniques. These two properties are normally difficult to achieve simultaneously in materials with Kerr-like nonlinearities, see [9].

To the best of our knowledge, walk-off effects on bright cavity solitons have not been addressed until now. Here we shall discuss them at a fundamental level using the optical parametric oscillator (OPO) as an example. Our main result is to demonstrate analytically and numerically how the common velocity of the mutually trapped two-component wave envelope is selected. In achieving this we will develop a method based on the evolution equations for the field momentum. This method gives a clear physical interpretation of the velocity selection mechanism and provides good quantitative estimates for the velocity itself. The timeliness of addressing this problem for cavity solitons stems in part from the ever-improving experimental results on observation of spatial and temporal localization effects and instabilities in $\chi^{(2)}$ cavities [15–17].

Assuming phase matching, the equations describing a synchronously pumped-pulsed ring OPO can be written in the following dimensionless form [11,12]:

$$\begin{aligned} -i(\partial_t + \gamma_1)E_1 &= (\alpha_1 \partial_z^2 + iv_1 \partial_z + \delta_1)E_1 + (E_2 + \mu)E_1^*, \\ -i(\partial_t + \gamma_2)E_2 &= (\alpha_2 \partial_z^2 + iv_2 \partial_z + \delta_2)E_2 + E_1^2. \end{aligned} \quad (1)$$

Here E_j , $j=1,2$ are the scaled, slowly varying envelopes of the intracavity fields at fundamental (signal) and second harmonic (pump) frequencies; explicit formulas connecting them to physical fields can be found in [11–13]. Dimensionless coordinates z and t can be interpreted, respectively, as the position measured in the frame moving with an average group velocity and time measured in the units of the cavity round trip. It is important to note that in deriving Eq. (1), the external pump field characterized by the parameter μ has been subtracted from the intracavity pump field, transforming to zero the cw solution corresponding to subthreshold behavior, see [12,14] for details. The coefficients δ_j and $\gamma_j \geq 0$ represent detunings from the cavity resonances and linear losses, respectively. The group velocity dispersion parameters α_j are taken to be $1/j$ in our numerical calculations. The walk-off parameters are $v_{1,2}$. We assume below, without loss of generality, that $v_2 = 0$.

We seek cavity solitons in the form $E_j = A_j(\tau)$, where $\tau \equiv z - Vt$, and velocity V is the unknown parameter characterizing common shift of the group velocities. The envelope profiles A_j obey the following set of ordinary differential equations:

$$\begin{aligned} -i\gamma_1 A_1 &= (\alpha_1 \partial_\tau^2 + i(v_1 - V)\partial_\tau + \delta_1)A_1 + (A_2 + \mu)A_1^*, \\ -i\gamma_2 A_2 &= (\alpha_2 \partial_\tau^2 - iV\partial_\tau + \delta_2)A_2 + A_1^2. \end{aligned} \quad (2)$$

For $v_1 = 0$, quiescent ($V = 0$) bright soliton solutions of Eqs. (1) and (2) existing in the region of bistability between the trivial ($E_j = 0$) and nontrivial homogeneous ($E_j = \text{const}_j$) solutions were studied in Refs. [10–12]. The trivial and two nontrivial solutions coexist if $\mu_L < \mu < \mu_R$ providing that $\delta_1 \delta_2 > \gamma_1 \gamma_2$, where $\mu_R = \sqrt{\delta_1^2 + \gamma_1^2}$ and $\mu_L = |\gamma_1 \delta_2 + \gamma_2 \delta_1| / \sqrt{\delta_2^2 + \gamma_2^2}$. The eigenvalue that determines the stability of the trivial solution of Eqs. (1) with respect to perturbations $\sim e^{\lambda t + ikz}$ is $\lambda = -\gamma_1 + ikv_1 + \sqrt{\mu^2 - (\delta_1 - k^2)^2}$. Be-

low we focus on the case when $\delta_1 < 0$ and the trivial solution loses its stability exactly at $\mu = \mu_R$. Furthermore, certain localization effects in models that go beyond the mean field approximation and include walk off were described in [18,19]. One can envisage that for $v_1 \neq 0$ practically any solution existing for $v_1 = 0$ should start to drift. It remains unclear, however, whether such moving structures can be found as solutions of the simple autonomous model (2) or whether they might belong to more complicated classes of non-steady moving solutions to Eqs. (1). Our primary objective here is to show how a family of the cavity solitons existing in the bistability region can be continued as steadily moving structures into the region of nonzero walk off.

A useful property of Eqs. (1) is that solitary solutions can be found in the limit when cavity losses γ_j are small, which physically corresponds to the limit of large cavity detunings [12]. Therefore, for the question of existence, the balance between nonlinear focusing and diffraction appears to be more crucial than the energy balance between external driving and loss. This relative importance, together with the absolute necessity of the latter balance, allows us to develop a physical reasoning for the selection of V based on the quasi-conservation of transverse momentum.

Specifically, straightforward manipulation of Eqs. (1) shows that the total field momentum $M = M_1 + M_2$ obeys

$$\partial_t M = -2\gamma_1 M_1 - 2\gamma_2 M_2, \quad (3)$$

where $M_j = -i \int dz (E_j^* \partial_z E_j - \text{c.c.})$ are momenta of the individual components. If the right-hand side of Eq. (3) is small, then M is a quasiconserved quantity, and one can assume that V is a slowly varying *order* parameter, $\partial_t V \ll 1$. To first approximation, Eq. (3) then becomes

$$\partial_t V \partial_V M = -2\gamma_1 M_1(V) - 2\gamma_2 M_2(V), \quad (4)$$

where $M_{1,2}$ represent the individual momenta calculated for $\gamma_{1,2} = 0$. For zero losses we have been able to numerically continue quiescent solutions [12] into the region of nonzero v_1 and V , by continuously increasing the latter (more reasoning on why it is possible will be given below). Thus M_j on the right-hand side of Eqs. (4) can be considered as continuous functions of the parameter V , as is the case in other similar Hamiltonian models [1–4]. Hence, for cavity solitons traveling with constant velocity one finds that

$$\frac{M_1(V)}{M_2(V)} = -\frac{\gamma_2}{\gamma_1}. \quad (5)$$

Therefore, if this equality holds, walking cavity solitons exist and travel with velocity selected by the ratio of losses of the fundamental and second harmonic fields. Plots in Fig. 1(a) show how $M_{1,2}$ depends on V , and hence the range of V for the possible existence of cavity solitons according to the formula (5). Note that a particular value of V can be selected only from the finite interval $V_{b2} \leq V \leq V_{b1}$, where $M_m(V_{bm}) = 0$, and it is strictly fixed by the ratio of losses. The dotted curves in Fig. 1(b) show the predicted dependence of V on γ_2/γ_1 , obtained using Eq. (5). Remarkably, in spite of the fact that the two-component cavity soliton moves

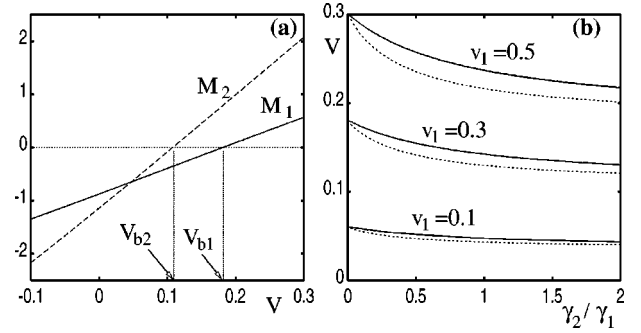


FIG. 1. (a) $M_{1,2}$ vs V for $\gamma_{1,2}=0$ and $v_1=0.3$. (b) V vs γ_2/γ_1 . Other parameters are $\delta_{1,2} = -2$, $\mu = 0.25$. Full lines corresponds to the numerical solution of Eqs. (2) and dotted lines are obtained from Eq. (5). All quantities in this and subsequent figures are dimensionless.

as a whole with selected velocity, its components carry momenta with opposite signs. Thus the walk-off compensating mechanism can be considered as analogous to the formation of excitons in semiconductors.

In order to independently verify the above considerations and to extend them to large γ 's we have used numerical path-following techniques to compute localized solutions to Eqs. (2) with V assumed unknown. We have found good agreement between the numerical and semianalytical results over a wide range of possible values of parameters, e.g., see Fig. 1(b). Figure 2 shows typical transverse profiles of the components and the interval of existence of single-humped solitons as the pump parameter μ is varied [Fig. 3(b) shows the corresponding variation of V]. Note that broad features of the profiles and parameter regions of existence are relatively insensitive to the value of v_1 . We have stopped computing solutions at a point where the branch of single-humped solitary waves undergoes a limit point (fold) at the large- μ end of their interval of existence (finite $|A_j|^2$). Computations can be continued beyond this point but the soliton profiles become multihumped, just as they do in the quiescent case [12]. Our numerical results reveal that the soliton profiles are asymmetric and that the degree of asymmetry is accentuated as one approaches the right-hand limit point of μ -interval of their existence, see Fig. 2(b) which is at just such a limit point.

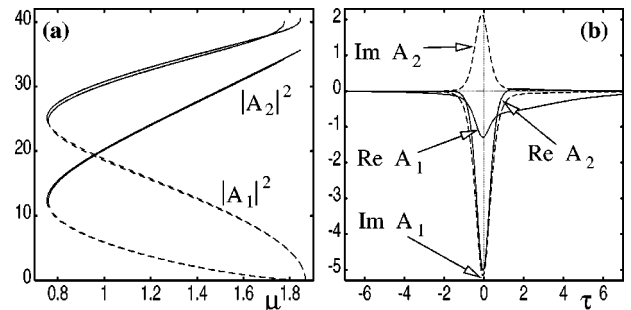


FIG. 2. (a) $\int d\tau |A_{1,2}|^2$ against pump parameter μ for $v_1=0.1$ and $v_1=1.0$ (almost overlaid) solid curves represent the stable portions of the branch. (b) Soliton profile for $v_1=0.5$, $\mu=1.821581$, which is just the right-most point of the existence region. Other parameters are $\delta_1 = -1.8$, $\delta_2 = -4$, $\gamma_{1,2} = 0.5$.

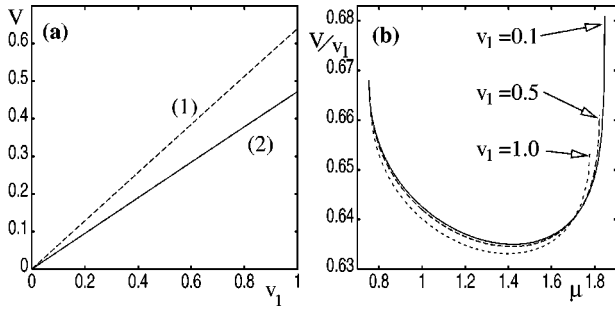


FIG. 3. (a) V against v_1 for: (1) $\gamma_{1,2}=0.5$, $\delta_1=-1.8$, $\delta_2=-4$, $\mu=1.0$; (2) $\gamma_{1,2}=0.02$, $\delta_{1,2}=-2$, $\mu=0.25$. (b) V/v_1 vs μ for $\gamma_{1,2}=0.5$, $\delta_1=-1.8$, $\delta_2=-4$.

To gain insight into the *dynamics* of the solitons in the presence of walk off, let us consider the effect that small

$$\hat{\mathcal{L}} \equiv \begin{bmatrix} -\gamma_1 - (v_1 - V)\partial_\tau - \text{Im}A_2 & \text{Im}A_1 & -\alpha_1\partial_\tau^2 - \delta_1 & -\text{Re}A_1 \\ -2\text{Im}A_1 & -\gamma_2 + V\partial_\tau & -2\text{Re}A_1 & -\alpha_2\partial_\tau^2 - \delta_2 \\ \alpha_1\partial_\tau^2 + \delta_1 + \text{Re}A_2 + \mu & \text{Re}A_1 & -\gamma_1 - (v_1 - V)\partial_\tau + \text{Im}A_2 & \text{Im}A_1 \\ 2\text{Re}A_1 & \alpha_2\partial_\tau^2 + \delta_2 & -2\text{Im}A_1 & -\gamma_2 + V\partial_\tau \end{bmatrix} \quad (7)$$

and $\vec{\xi} = (u_1, u_2, w_1, w_2)^T$. This mode is given by the gradient of the cavity soliton $\vec{\xi}_0 = \partial_\tau(\text{Re}A_1, \text{Re}A_2, \text{Im}A_1, \text{Im}A_2)^T$ and Eq. (7) has been derived by substituting the ansatz

$$E_j = A_j(\tau) + \epsilon[u_j(\tau, t) + iw_j(\tau, t)] \quad (8)$$

into Eqs. (1) and assuming $\epsilon \ll 1$, $u_j, w_j \sim e^{\lambda t}$.

For zero losses, our system becomes Hamiltonian and the soliton's position obeys Newton's equation for a free particle, $\partial_\tau^2 z_0 = 0$. This explicitly shows that the translational mode $\vec{\xi}_0$ is now doubly degenerate and that velocity of the soliton is an arbitrary parameter determined by initial conditions. Note that the losses introduce not only damping [the term proportional to $\partial_\tau z_0$ in Eq. (6)] into the soliton dynamics as one might expect, making $\lambda_\gamma < 0$, but also external forcing (the term proportional to V_s). Numerical analysis of the spectrum of $\hat{\mathcal{L}}$ has shown that the region of stability of the walking solitons is approximately inherited from the quiescent case [12]. This region of stability is as indicated by the solid lines in Fig. 2 (b), where for these moderately large γ values the Hopf bifurcation, present in the Hamiltonian limit $\gamma_{1,2} \rightarrow 0$ at μ values to the left of the right-hand limit point, has been suppressed.

To explicitly calculate the dependence of V on v_1 , we take the new limit of small $v_1 = \epsilon$ and seek solution of Eqs. (1) in the form (8), where $\tau = z - z_0(t)$ and $\partial_\tau z_0 \sim \epsilon$. We find that to the first order: $\epsilon(\hat{\mathcal{L}}_0 - \partial_\tau)\vec{\xi} = \partial_\tau z_0 \vec{\xi}_0 - v_1 \vec{\mathcal{P}}$, where $\hat{\mathcal{L}}_0 = \hat{\mathcal{L}}(v_1 = V = 0)$ and $\vec{\mathcal{P}} = \partial_z(\text{Re}E_1, \text{Im}E_1, 0, 0)^T$. V is found from the

dissipation has on the spectral properties of walking solitons. For this purpose it is useful to deduce from Eq. (4) the equation for the soliton position $z_0 = \int^t V(t') dt'$. Expanding the right-hand side of Eq. (4) in Taylor series about $V = V_s$, where V_s is found from Eq. (5), one obtains

$$M' \partial_\tau^2 z_0 = 2(\gamma_1 M'_1 + \gamma_2 M'_2)(V_s - \partial_\tau z_0), \quad (6)$$

where $'$ stands for derivative with respect to V at $V = V_s$. The same equation can also be derived by direct asymptotic expansion, see below. Analyzing the stability of the solution $z_0 = V_s t$ we find that it has eigenvalues $\lambda_\gamma = -2(\gamma_1 M'_1 + \gamma_2 M'_2)/M'$ and $\lambda_z = 0$. The latter corresponds to the zero-eigenvalue (translational) mode of the eigenvalue problem $\hat{\mathcal{L}}\vec{\xi} = \lambda\vec{\xi}$, where

$$\langle \vec{\xi}_0, \vec{\xi}_0^\dagger \rangle V = v_1 \langle \vec{\mathcal{P}}, \vec{\xi}_0^\dagger \rangle, \quad (9)$$

which explicitly shows proportionality of V to v_1 . Here $\vec{\xi}_0^\dagger$ is the translational mode of the adjoint operator, $\hat{\mathcal{L}}^\dagger \vec{\xi}_0^\dagger = 0$, and $\langle \cdot, \cdot \rangle$ defines scalar product. It is clear now that the effective external force in Eq. (6) is proportional not only to losses but, unlike the effective friction, to v_1 also. Fig. 3(a) shows numerically calculated dependence of V vs v_1 , indistinguishable on the scale depicted from the results obtained from Eq. (9), namely, $V/v_1 = 0.645$ and 0.475 for the parameter cases (1) and (2), respectively. Surprisingly, even for $v_1 \sim 1$ the linear dependence predicted by Eq. (9) is preserved to within a few percent. Dependence of V/v_1 on the pump parameter in Fig. 3(b) shows that V varies only slightly with μ over the stable part of the branch, with the variation being the greatest near the ends of the μ interval. Furthermore, numerical calculations over a range of other parameter values have indicated that V_s never exceeds v_1 . Equation (9) starts to give poor results when $\langle \vec{\xi}_0, \vec{\xi}_0^\dagger \rangle$ becomes the order of ϵ , which happens in the Hamiltonian limit $\gamma_{1,2} \sim \epsilon$. In this case one needs to assume $v_1 \sim \epsilon^2$ and proceed with an asymptotic expansion up to second order. In fact, this second-order term gives nothing other than Eq. (6), and signals that Eqs. (3) and (6) should be considered as having second order of smallness in ϵ . Note that finding explicit expressions for the effective mass M' and friction λ_γ is more cumbersome using this asymptotic approach, compared to our previous momentum-based method. Nevertheless, the two methods give the same final answer.

The question of velocity selection can also be approached from a more intuitive, symmetry-based point of view. Upon taking small perturbations of the trivial zero solution of Eqs. (2) proportional to $e^{\omega\tau}$, one can show that the eigenvalues ω are roots of the characteristic polynomial $\chi(\omega) = [(\alpha_1\omega^2 + \delta_1)^2 + ((v_1 - V)\omega + \gamma_1)^2 - \mu^2][(\alpha_2\omega^2 + \delta_2)^2 + (\gamma_2 - V\omega)^2]$. Inside the region of the soliton existence χ has four roots whose real parts are positive and four roots with negative real parts. Generically therefore, in order for the four-dimensional stable and unstable manifolds to intersect along a homoclinic orbit [corresponding to a solitary-wave solution to Eqs. (1)] one needs to tune one of the parameters, e.g., velocity V , to a particular value, while holding the other parameters fixed. Thus walking cavity solitons are a *codimension-one* phenomenon in the parameter space of Eqs. (2).

There are, however, two special limits in which the solitons acquire special symmetries and, as a consequence of this, a lower codimension. The first is if $\gamma_{1,2} = 0$. Then Eqs. (2) become invariant with respect to reversibility transformation

$$R_1 : (\tau, \text{Re } A_1, \text{Im } A_1, \text{Re } A_2, \text{Im } A_2) \\ \rightarrow (-\tau, -\text{Re } A_1, \text{Im } A_1, \text{Re } A_2, -\text{Im } A_2), \quad (10)$$

and we find that a family of R_1 -symmetric solitons exist for a continuous V -interval, i.e., have *codimension zero*. This is because, intersection of the stable and unstable manifolds now automatically takes place if trajectories leaving zero along the four-dimensional unstable manifold intersect the four-dimensional symmetry hyperplane $\text{fix}(R_1)$ at a point. A second limit is the case of quiescent solitons $v_1 = V = 0$, when Eqs. (2) are invariant under a different reversibility, $R_2 : (\tau, A_1, A_2) \rightarrow (-\tau, A_1, A_2)$. Then R_2 -symmetric codimension-zero solitons exist throughout a finite range of parameters [12]. Thus both of the asymptotic methods applied above are valid in the limits when either of the symmetries R_1 or R_2 are weakly broken. Therefore, it would be correct to interpret velocity selection as being due to the breaking of reversibility. For a review of properties of the homoclinic orbits in reversible systems see, e.g., [20].

Finally we verify the velocity selection mechanism and the stability of the walking solitons by presenting the results of numerical simulation of Eqs. (1). First we consider excitation of a solitary structure in the presence of the walk-off and with zero losses. If localized initial conditions are even functions of z , i.e., the initial momentum is zero, then, providing that walk-off is nonzero, emission of linear waves during the relaxation to the solitary wave has an asymmetric character and therefore the emerging soliton acquires non-zero velocity, see Fig. 4(a). Walk-off-induced momentum transfer from linear waves to solitons can be compensated by imposing asymmetric transverse variations of the phase of the initial conditions. Thus, the soliton velocity is a tunable parameter and can be reduced, e.g., to zero, see Fig. 4(b). In contrast, when we take into account losses, then, the simulations clearly show that the soliton's velocity becomes independent of the value of the momentum stored in the initial

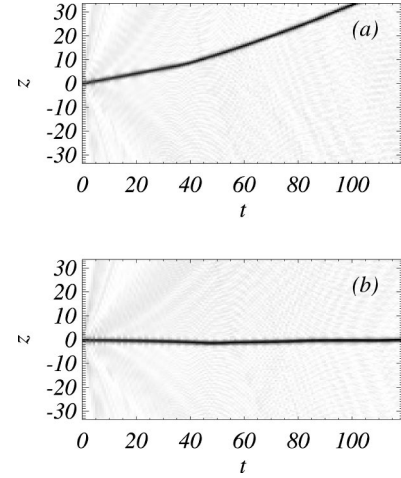


FIG. 4. Trajectories of walking cavity solitons after excitation by localized initial conditions: $E_{1,2} = a_{1,2} \exp(-z^2/w^2 + i\alpha_{1,2}z)$. (a) $\alpha_{1,2} = 0$, (b) $\alpha_{1,2} = -0.2$. Other parameters $v_1 = 0.2$, $\gamma_{1,2} = 0$, $\mu = 0.5$, $\delta_{1,2} = -2$, $a_1 = 10$, and $a_2 = 1$.

conditions, see Fig. 5. This is in full agreement with the above analytical considerations.

Let us also remark briefly on previous studies involving velocity selection. In reaction-diffusion systems arising in biology and chemistry, the notion of the selection of the speed of a front or pulse is widespread; in, e.g., the FitzHugh-Nagumo equations for nerve impulses [21], or the nonlinear Schrödinger equation with third-order dispersion and dissipative corrections [22]. Note, that in the latter work an approach based on energy and momentum balance similar to the one described above was used to find the selected value of the soliton velocity. In the context of quadratic nonlinearity, dissipative shock waves, and solitons in the presence of walk-off have recently been modeled using so-called quadratic Ginzburg-Landau (GL) equations [23,24]. Walking domain walls in optical parametric oscillators above threshold have been reported in [25] using a reduction of Eqs. (1) to a real GL equation. Also, questions of pattern formation in the presence of walk off have attracted much attention recently, see, e.g., [13,26].

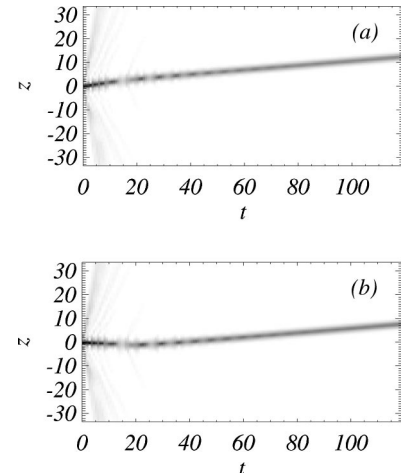


FIG. 5. The same as Fig. 4, but $\gamma_{1,2} = 0.05$.

In summary, we have established the existence of two-component cavity solitons in the degenerate OPO with walk-off and have revealed the phenomenon of velocity selection. Moreover, we have provided asymptotic methods for predicting the selected velocity of dissipative solitons, for which we get excellent numerical agreement. These methods, valid in the limits of small losses or walk-off, can be generalized to other multicomponent optical systems. Moreover, we have shown how the asymptotic results can be interpreted in terms

of the breaking of reversibility by the inclusion of walk off and losses. We finally remark that we have also obtained results similar to the above for nondegenerate OPOs, where not only velocity, but also frequency shift is selected [27], and for the case of two-dimensional spatial solitons.

We thank W.J. Firth for useful discussions. DVS acknowledges support from the Royal Society of Edinburgh and the EPSRC Grant No. GR/N19830.

-
- [1] L. Torner, D. Mazilu, and D. Mihalache, *Phys. Rev. Lett.* **77**, 2455 (1996).
- [2] C. Etrich, U. Peschel, F. Lederer, and B.A. Malomed, *Phys. Rev. E* **55**, 6155 (1997).
- [3] D. Mihalache, D. Mazilu, L.-C. Crasovan, and L. Torner, *Phys. Rev. E* **56**, R6294 (1997).
- [4] D. Mihalache, D. Mazilu, and L. Torner, *Phys. Rev. Lett.* **81**, 4353 (1998).
- [5] W. Torruellas, Z. Wang, D.J. Hagan, E.W. VanStryland, G.I. Stegeman, L. Torner, and C. R. Menyuk, *Phys. Rev. Lett.* **74**, 5036 (1995).
- [6] X. Liu, K. Beckwitt, and F. Wise, *Phys. Rev. E* **62**, 1328 (2000).
- [7] W.J. Firth and G.K. Harkness, *Asian J. Phys.* **7**, 665 (1998).
- [8] C. O. Weiss, G. Sleky, V. B. Taranenko, K. Staliunas, and R. Kuszelewicz, <http://xxx.lanl.gov/nlin.PS/0003015>.
- [9] S. A. Akhmanov, V. A. Vysloukh, and A. S. Chirkin, *Optics of Femtosecond Laser Pulses* (Springer, New York, 1992), Chap. 2.
- [10] K. Staliunas and V.J. Sánchez-Morcillo, *Opt. Commun.* **139**, 306 (1997).
- [11] S. Trillo and M. Haelterman, *Opt. Lett.* **23**, 1514 (1998).
- [12] D.V. Skryabin, *Phys. Rev. E* **60**, R3508 (1999).
- [13] M. Santagiustina, P. Colet, M. San Miguel, and D. Walgraef, *Phys. Rev. E* **58**, 3843 (1998).
- [14] G.-L. Oppo *et al.*, *J. Mod. Opt.* **41**, 1151 (1994); S. Longhi, *Phys. Rev. A* **53**, 4488 (1996).
- [15] D.T. Reid, J.M. Dudley, M. Ebrahimzadeh, and W. Sibbett, *Opt. Lett.* **19**, 825 (1994).
- [16] M. Vaupel, A. Maitre, and C. Fabre, *Phys. Rev. Lett.* **83**, 5278 (1999).
- [17] A. Mamaev and M. Saffman (unpublished).
- [18] A.J. Scroggie, G.D. Alessandro, and G.-L. Oppo, *Opt. Commun.* **160**, 119 (1999).
- [19] P.S. Jian, W.E. Torruellas, M. Haelterman, S. Trillo, U. Peschel, and F. Lederer, *Opt. Lett.* **24**, 400 (1999).
- [20] A.R. Champneys, *Physica D* **112**, 158 (1998).
- [21] Y. A. Kuznetsov, *Elements of Applied Bifurcation Theory* (Springer, New York, 1998), Chap. 6.3 and references therein.
- [22] B.A. Malomed, I.M. Uzunov, M. Gölles, and F. Lederer, *Phys. Rev. E* **55**, 3777 (1997).
- [23] S. Darmanyan, A. Kamchatnov, and F. Lederer, *Phys. Rev. E* **58**, R4120 (1998).
- [24] L.-C. Crasovan, B.A. Malomed, D. Mihalache, D. Mazilu, and F. Lederer, *Phys. Rev. E* **62**, 1322 (2000).
- [25] J.N. Kutz, T. Erneux, S. Trillo, and M. Haelterman, *J. Opt. Soc. Am. B* **16**, 1936 (1999).
- [26] M. Santagiustina, P. Colet, M. San Miguel, and D. Walgraef, *Opt. Lett.* **23**, 1167 (1998).
- [27] D.V. Skryabin, A.R. Champneys, and W.J. Firth, *Phys. Rev. Lett.* **84**, 463 (2000).